06.5

The structure of the contact zone of the surfacing–substrate subjected to electron-beam processing

© Yu.F. Ivanov[1], V.E. Gromov[2], M.O. Efimov[2], Yu.A. Shliarova[2], I.A. Panchenko[2], S.V. Konovalov[2]

[1] Institute of High Current Electronics, Siberian Branch, Russian Academy of Sciences, Tomsk, Russia
[2] Siberian State Industrial University, Novokuznetsk, Russia
E-mail: gromov@physics.sibsiu.ru

Received November 2, 2022
Revised January 10, 2023
Accepted January 11, 2023

Using scanning and transmission electron microscopy, the analysis of the structure, phase and elemental composition of the contact zone of the system coating (high-entropy FeCrCoNiMn alloy)–substrate (5083 alloy) after electron-beam processing was performed. The formation of a multiphase, multielement submicro- and nanocrystalline structure has been established. The structure of high-speed cellular crystallization in the contact layers adjacent to the coating and substrate is revealed, and the formation of lamellar crystals in the central region of the contact zone is also found. Keywords: contact zone, high-entropy alloy, wire-arc additive manufacturing method, 5083 aluminum alloy, pulsed electron beam, elemental and phase composition, structure..

Keywords: contact zone, high-entropy alloy, wire-arc additive manufacturing method, 5083 aluminum alloy, pulsed electron beam, elemental and phase composition, structure.

DOI: 10.21883/TPL.2023.03.55689.19410

In the past two decades, the examination of novel high-entropy alloys (HEAs), which consist of five or more elements with a concentration of 5–35 at.%, has held a special place [1–4] in current material physics, since these alloys have exceptional functional properties (wear and corrosion resistance, mechanical characteristics at low and high temperatures, unique magnetic properties, etc.) [5,6]. Reviews [1,2,7–12] are focused on analyzing the structural and phase states, the defect substructure, and the stability of HEAs; the methods of their production; and potential practical applications of such alloys. The use of high-entropy coatings instead of bulk HEAs allows one to reduce the cost of articles and expand the range of their application [12,13]. Various processing methods are used to improve the surface properties of HEAs [14]. Electron-beam processing is one of the promising and highly efficient surface modification techniques [15]. It provides ultrahigh rates of surface heating (up to 10^8 K/s) and cooling via heat extraction into the bulk of the material. Non-equilibrium submicro- and nanocrystalline structural and phase states emerge as a result, and the chemical composition becomes more homogeneous [15].

The aim of the present study is to examine the effect of electron-beam processing on formation of the structure of the contact zone in the HEA coating (FeCrCoNiMn)–substrate (5083 alloy) system using electron microscopic techniques.

Samples of the coating–substrate system were studied. The coating is a high-entropy Cantor alloy with a non-equiatomic FeCrCoNiMn elemental composition (at.%: Fe — 37.9, Cr — 14.9, Co — 25.0, Ni — 17.9, Mn — 3.5, and the rest is impurities), which was produced on a substrate by wire-arc additive manufacturing [3,4]. The substrate was made of an aluminum-based 5083 alloy. The „SOLO“ setup (Institute of High Current Electronics, Siberian Branch, Russian Academy of Sciences) was used to irradiate the contact zone of the coating–substrate system by a high-intensity pulsed electron beam. The process parameters were as follows: energy $U = 18$ keV of accelerated electrons, electron-beam energy density $E_S = 30\,\mathrm{J/cm^2}$ at pulse duration $t = 200\,\mu$s, number of pulses $N = 3$, and pulse repetition rate $f = 0.3\,\mathrm{s}^{-1}$. These experiments were carried out in vacuum under residual gas (argon) pressure $p = 0.02$ Pa in the working chamber. Scanning (SEM 515 Philips with an EDAX ECON IV electron microprobe analyzer) and transmission (JEM-2100) electron microscopy techniques were used to examine the elemental and phase composition and the state of the defect substructure of the coating–substrate contact zone [16–18]. Cross-section samples for transmission electron microscopy (TEM) were prepared in accordance with the classical procedure [18], which involves mechanical processing (gluing, sanding, and polishing) and etching by Ar^+ ions with an energy of 4–5 keV at Ion Slicer EM-091001S (Joel, Japan).

Figure 1, *a* presents an example SEM (scanning electron microscopy) image of the cross section of the zone of contact between the HEA coating and the substrate (5083 Al/Mg $\sim 92.4/5.7$ at.% alloy) after electron-beam processing. The formation of an intermediate layer with a thickness up to 700 μm, which is characterized by microcracking along the substrate–intermediate layer interface, is evident. The contact layer has curving boundaries, which

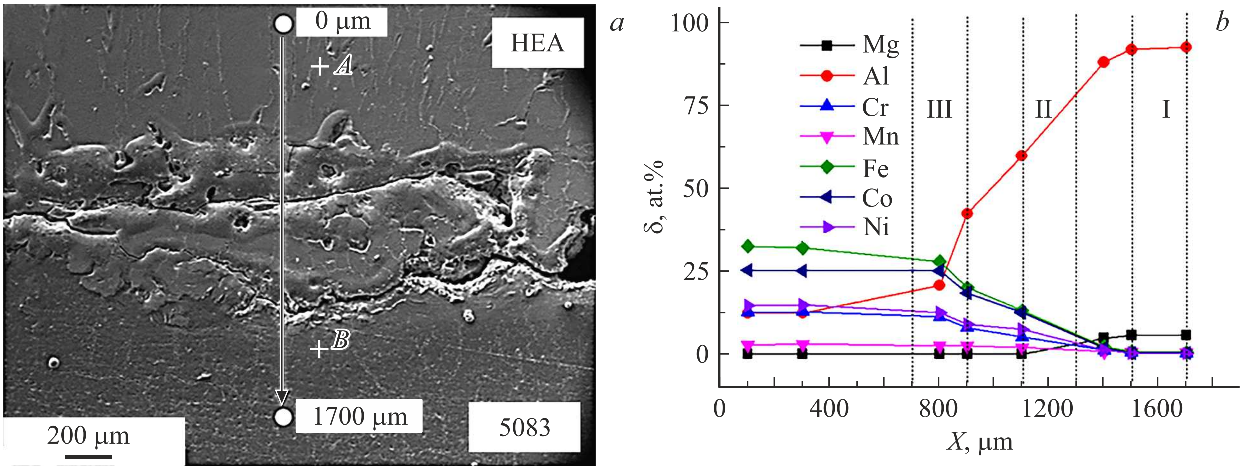

Figure 1. 1. SEM image of the cross section (*a*) and composition profile determined by EMPA (*b*) for the HEA coating (FeCrCoNiMn) (region *A*)–substrate (5083 alloy) (region *B*) structure formed as a result of electron-beam processing. Numbers I, II, and III denote the layers in which TEM studies of the structure and phase composition of the alloy were performed.

Results of electron microprobe analysis of the elemental composition (at.%) of the coating in region *A* and the substrate in region *B*

Region	Element						
	Mg	Al	Cr	Mn	Fe	Co	Ni
A	0	12.3	12.6	2.7	32.5	25.3	14.6
B	5.7	92.4	0.3	0.5	0.5	0.3	0.3

may be indicative of a high level of alloying between the substrate and the deposited material.

The composition profile (Fig. 1, *b*) was determined by electron microprobe analysis (EMPA). This profile features three primary (HEA coating, substrate, and region with a composition gradient) and two intermediate (HEA coating–region with a composition gradient and region with a composition gradient–substrate transitions) regions. The characteristic sizes of the upper transition region, the region with a composition gradient, and the lower transition region are 200, 400, and 100 μm, respectively. The greater thickness of the upper transition region is indicative of higher aluminum diffusion rates [19].

It may be assumed that the process of mutual alloying of the coating and the substrate under irradiation by a pulsed electron beam leads to a significant alteration of the phase composition of the contact zone (see the table). TEM studies were performed for layers I, II, and III indicated in Fig. 1, *b*.

Layer I features structural cells 260–410 nm in size. The obtained images reveal that a solid solution of magnesium in aluminum (face-centered cubic lattice), which corresponds to a 5083 alloy, fills the volume of these cells. Crystallization cells are separated by Mg_2Si interlayers. Interlayers of the minor phase, which are located at the boundaries of cells, are enriched with atoms forming the deposited material and the substrate. Structures of this kind are often observed in the case of rapid cooling of metallic alloys [20]. The cellular structure degenerates into a lamellar one with distance from the zone of contact with the coating.

Layer II has a lamellar structure with $Al_{13}Fe_4$ (monoclinic lattice) and CrNiFe (face-centered lattice) being its primary phases. The transverse size of lamellae varies from 270 to 410 nm. Using the methods of foil EMPA, we found that aluminum is the primary element (76.8 at.%) in this layer. The following elements with lower concentrations were also identified: Mg (4.1 at.%), Cr (2.2 at.%), Mn (0.3 at.%), Fe (4.9 at.%), Co (1.6 at.%), and Ni (10.1 at.%).

Structural studies carried out with the use of dark-field images with indexing of electron microdiffraction patterns revealed that layer II is formed by the following phases: $Al_{13}Fe_4$, CrNiFe, and Al_6Fe.

An example TEM image of layer III is shown in Fig. 2, *a*. The layer structure is cellular in nature and corresponds to rapid crystallization [15]. Crystallites are 200–500 nm in size. A 0.17Mg–20.3Al–4.3Cr–16.7Fe–9.3Co–49.2Ni alloy, which corresponds to the HEA alloyed with substrate elements, fills the volume of cells. Interlayers of the minor phase located at the boundaries of cells are also formed by elements from the deposited material and the substrate (41.4Mg–10.9Al–9.0Cr–1.0 Mn–15.2Fe–4.1Co–18.4Ni).

Example dark-field TEM images of the indicated region are shown in Figs. 2, *b*, *c*. It follows from the analysis of dark-field images that a solid solution based on the HEA alloyed with aluminum and magnesium fills the volume of rapid crystallization cells (Fig. 2, *b*). Crystallization cells are separated by $Al_{18}Cr_2Mg_3$i interlayers (Fig. 2, *c*).

A HEA coating with a non-equiatomic FeCrCoNiMn elemental composition was formed on a 5083 alloy by wire-arc additive manufacturing. The influence of irradiation of the contact zone of the HEA coating–substrate (5083 alloy) by a high-intensity pulsed electron beam (up to 30 J/cm^2)

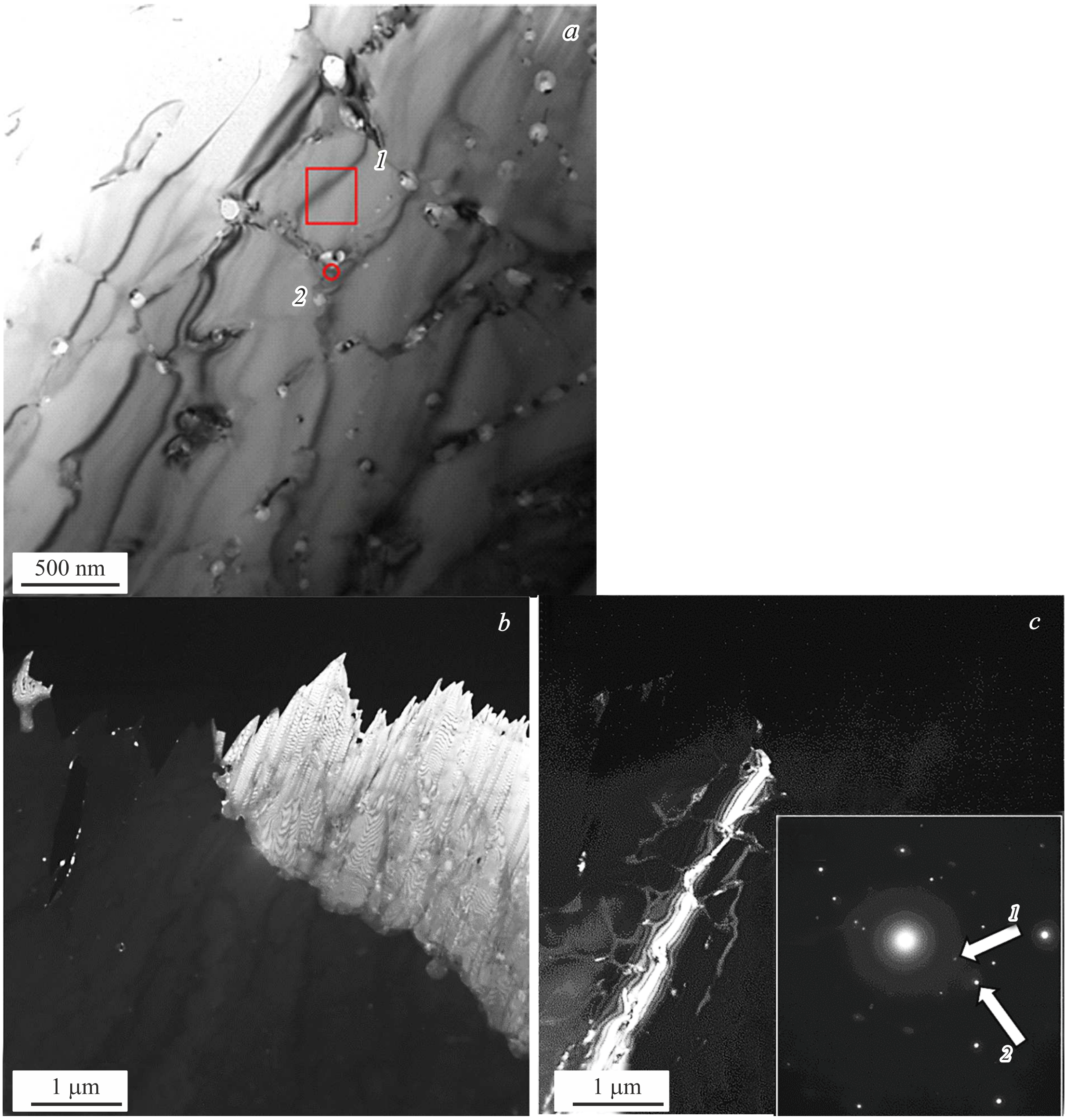

Figure 2. Results of TEM studies of the cross section of the HEA coating (FeCrCoNiMn)−substrate (5083 alloy) structure in the region of layer III: bright-field (*a*) and dark-field images in reflections 210 Cr−Ni−Fe (*b*) and 222 Cr−Ni−Fe + 880 $Al_{18}Cr_2Mg_3$ (*c*). The rectangle and the circle in panel *a* denote the sites where EMPA was performed. The electron diffraction pattern for the region shown in panel *a* is presented in the inset. Numbers in panel *a* and the inset denote the reflections corresponding to dark-field images in panels *b* (*1*) and *c* (*2*).

on the crystal structure and the composition distribution was examined. The elemental and phase composition and the state of the defect substructure of the coating−substrate contact zone were studied. Mutual alloying of the coating and the substrate in a layer with a thickness of $\sim 1700\,\mu$m was revealed. It was demonstrated that rapid cooling of the contact zone after processing by a pulsed electron beam results in the formation of a multielement and multiphase submicro- and nanocrystalline structure, which is typical of rapid cellular crystallization. A solid solution of magnesium in aluminum, which corresponds to the 5083 alloy composition, fills the volume of cells. Interlayers of the minor phase are located at the boundaries of cells and are enriched with atoms forming the substrate and the coating. A layer with a predominantly lamellar–cellular crystal structure and a composition gradient forms in the central region of the contact zone. The contact layer adjacent to the coating also has the structure typical of rapid cellular crystallization. A 0.17Mg−20.3Al−4.3Cr−16.7Fe−9.3Co−49.2Ni alloy, which corresponds to the HEA alloyed with substrate elements, fills the volume of cells. Interlayers of the minor phase, which are located at the boundaries of cells, are enriched with magnesium and, to a lesser extent, with atoms forming the coating.

Funding

The fabrication of coating (HEA)–substrate (5083 alloy) samples by wire-arc additive manufacturing and the examination of the contact zone by transmission electron microscopy were carried out with financial support from the Russian Science Foundation (project No. 20-19-00452), and experiments on irradiation of the coating–substrate system by a pulsed electron beam and SEM studies into the structure of the irradiated layer were supported by grant No. 19-19-00183 from the Russian Science Foundation (https://rscf.ru/project/19-19-00183/).

Conflict of interest

The authors declare that they have no conflict of interest.

References

[1] J.W. Yeh, S.K. Chen, S.J. Lin, J.Y. Gan, T.S. Chin, T.T. Shun, C.H. Tsau, S.Y. Chang, Adv. Eng. Mater., **6** (5), 299 (2004). DOI: 10.1002/adem.200300567
[2] B. Cantor, I.T.H. Chang, P. Knight, A.J.B. Vincent, Mater. Sci. Eng. A, **375-377**, 213 (2004). DOI: 10.1016/j.msea.2003.10.257
[3] V.E. Gromov, S.V Konovalov, Yu.F. Ivanov, K.A. Osintsev, *Structure and properties of high-entropy alloys* (Springer, 2021).
[4] V.E. Gromov, Yu.F. Ivanov, K.A. Osintsev, Yu.A. Shlyarova, I.A. Panchenko, *High-entropy alloy: structure and properties* (RuScience, M., 2022).
[5] K.K. Alaneme, M.O. Bodunrin, S.R. Oke, Mater. Res. Technol., **5** (4), 384 (2016). DOI: 10.1016/j.jmrt.2016.03.004
[6] W. Zhang, P.K. Liaw, Y. Zhang, Sci. China Mater., **61** (1), 2 (2018). DOI: 10.1007/s40843-017-9195-8
[7] Y. Zhang, T.T. Zuo, Z. Tang, M.C. Gao, K.A. Dahmen, P.K. Liaw, Z.P. Lu, Prog. Mater. Sci., **61**, 1 (2014). DOI: 10.1016/j.pmatsci.2013.10.001
[8] D.B. Miracle, O.N. Senkov, Acta Mater., **122**, 448 (2017). DOI: 10.1016/j.actamat.2016.08.081
[9] M.-H. Tsai, J.-W. Yeh, Mater. Res. Lett., **2** (3), 107 (2014). DOI: 10.1080/21663831.2014.912690
[10] B.S. Murty, J.W. Yeh, S. Ranganathan, P.P. Bhattacharjee, *High-entropy alloys*, 2nd ed. (Elsevier, Amsterdam, 2019).
[11] Y. Zhang, *High-entropy materials. A brief introduction* (Springer Nature, Singapore, 2019).
[12] A.S. Rogachev, Phys. Metals Metallogr., **121** (8), 733 (2020). DOI: 10.1134/S0031918X20080098.
[13] A.D. Pogrebnjak, A.A. Bagdasaryan, I.V. Yakushchenko, V.M. Beresnev, Russ. Chem. Rev., **83** (11), 1027 (2014). DOI: 10.1070/RCR4407.
[14] J. Guo, M. Goh, Z. Zhu, X. Lee, M.L.S. Nai, J. Wei, Mater. Design, **153**, 211 (2018). DOI: 10.1016/j.matdes.2018.05.012
[15] Yu.F. Ivanov, V.E. Gromov, D.V. Zagulyaev, S.V. Konovalov, Yu.A. Rubannikova, A.P. Semin, Prog. Phys. Met., **21** (3), 345 (2020). DOI: 10.15407/ufm.21.03.345
[16] F.R. Egerton, *Physical principles of electron microscopy* (Springer International Publ., Basel, 2016).
[17] C.S.S.R. Kumar, *Transmission electron microscopy. Characterization of nanomaterials* (Springer, N.Y., 2014).
[18] C.B. Carter, D.B. Williams, *Transmission electron microscopy* (Springer International Publ., Berlin, 2016).
[19] L.I. Larikov, V.I. Isaichev, *Diffuziya v metallakh i splavakh. Spravochnik* (Nauk. Dumka, Kiev, 1989) (in Russian).
[20] V.P. Rotshtein, D.I. Proskurovskii, G.E. Ozur, Yu.F. Ivanov, *Modifikatsiya poverkhnostnykh sloev metallicheskikh materialov nizkoenergeticheskimi sil'notochnymi elektronnymi puchkami* (Nauka, Novosibirsk, 2019) (in Russian).